Earthquake Geotechnical Engineering for Protection and Development of Environment and Constructions – Silvestri & Moraci (Eds)
© 2019 Associazione Geotecnica Italiana, Rome, Italy, ISBN 978-0-367-14328-2

Dynamic liquefaction analysis of a tailings dam in Peru

P.J. Pinedo, J.R.C. Huertas & C. Romanel
Department of Civil and Environmental Engineering, Pontifical Catholic University of Rio de Janeiro, Rio de Janeiro, Brazil

ABSTRACT: This work investigates the seismic behavior of a tailings dam that will be raised by the center line method in a region of high seismic activity in Peru. Numerical analysis was performed to verify the liquefaction potential of the tailings, considering the UBC-Sand and Byrne constitutive models for cyclic loading generated by an earthquake of magnitude M_w = 8.2. The results of the analyzes are presented in terms of the pore pressure parameter r_u as well as maximum permanent displacements in the tailings deposit. Although the fine tailings exhibit dynamic li-quefaction potential, the stability of the rockfill dam does not seem to be in jeopardy.

1 INTRODUCTION

Peru is a country of high mineral exploitation, requiring the construction of dams for tailings storage, generally saturated materials with low relative density. One of the most critical problems in the performance of these structures is the dynamic behavior under high intensity seismic loads. Dynamic behavior means not only the overall stability of the dam but also the development of pore pressure that may induce the tailings liquefaction, a phenomenon characterized by loss of stiffness and strength for a short time, but sufficient to cause instability problems. Examples of the occurrence of dynamic liquefaction in tailings deposits were the El Cobre dam, Chile, in 1965 (Venegas, 2011), the Tapo Canyon tailings deposit in the United States, in 1994 (Harder and Stewart, 1996), the Amatista tailings dam, Peru, in 1996 (Mantegh, 2006) and the tailings deposit Las Palmas, Chile, in 2010 (Verdugo and González, 2015).

The objective of this paper is to estimate the dynamic liquefaction potential of a tailings dam in Peru under a seismic loading generated by an earthquake of magnitude M_w = 8.2, with similar characteristics to the earthquake occurred in the city of Arequipa, on June 23rd, 2001, with epicentral distance of 682 km to the dam site (Tavera, 2002). The earthquake's original accelerogram was adjusted to the uniform hazard spectrum obtained from the local seismic hazard study.

The geometry of the cross-section of the tailings dam is shown in Figure 1, already raised from the elevation 4043 m (current configuration) to elevation 4100 m above sea level (projected configuration). According to recommendations of the Canadian Dam Association (CDA, 2013), the tailings dam hazard classification is high, after considering the population at risk and the incremental losses in infrastructure, economics and environment as a consequence of an eventual co-llapse of the structure. Hence, the dynamic analyses were carried out considering a safety evaluation earthquake (SEE) with a return period of 2475 years and peak horizontal acceleration PHA = 0.40 g.

2 MATERIAL PROPERTIES

Materials properties were evaluated through several site investigations (standard penetration tests, trial pits, dynamic probing light, Lugeon or Packer tests, Lefranc tests, electrical

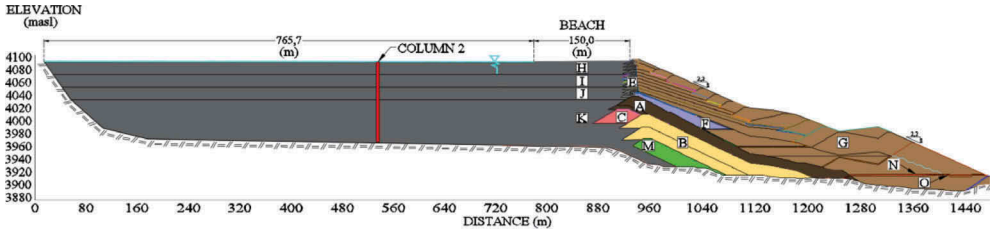

Figure 1. Cross section of the tailings dam after raising to elevation 4100 m above sea level.

Table 1. Geotechnical properties of granular materials represented by the Mohr-Coulomb model.

Material	Description	υ	E MPa	γ kN/m^3	c‘ kPa	ϕ‘	n	k m/s
A	Existing rockfill	0.33	$1.1x10^3$	22.0	0.0	40.0	0.25	$1.0x10^{-4}$
B	Granular embankment	0.30	$2.8x10^3$	20.5	0.0	35.0	0.35	$2.0x10^{-5}$
C	Old waste	0.30	$2.2x10^3$	21.0	0.0	36.0	0.40	$1.0x10^{-5}$
D	Rock	0.15	$5.4x10^4$	22.5	-	-	0.20	$1.0x10^{-9}$
E	Strutural embankment 1	0.30	$2.4x10^3$	20.0	5.0	35.0	0.40	$1.0x10^{-5}$
F	Strutural embankment 2	0.30	$2.2x10^3$	21.0	0.0	35.0	0.40	$5.0x10^{-4}$
G	New rockfill	0.33	$3.1x10^3$	22.0	0.0	40.0	0.25	$9.0x10^{-4}$
N	Filter	0.33	$2.2x10^3$	19.5	0.0	35.0	0.50	$5.0x10^{-4}$
O	Geomembrane	0.28	$1.7x10^3$	18.0	0.0	25.0	0.10	$1.0x10^{-11}$

resistivity and seismic refraction tests) as well as laboratory tests (particle-size distribution, Atterberg limits, consolidated undrained triaxial compression tests, point load tests, flexible and rigid wall per-meability tests). Table 1 lists the values of the geotechnical properties of the various soil layers, identified by letters A to O, as indicated in Figure 1. The Mohr-Coulomb constitutive model was selected to represent the mechanical behavior of materials A, B, C, E, F, G, N and O and the linear elastic model was chosen for the mechanical behavior of the rock bedding (material D). The fine tailings are basically characterized as loose silty sands with 19% fines and its mechanical beha-viour was simulated considering the Byrne (1991) and UBCSand (Byrne et al., 1995; Byrne et al., 2004) constitutive soil models, both implemented in the FLAC 2D v.8 software (Itasca, 2016), whose respective parameters are shown in Table 2. Laboratory tests were not performed to calibrate the parameters of the Byrne and

Table 2. Geotechnical properties of tailings represented by the Byrne and UBCSand models.

Model	Parameter	H	I	J	K	M
Byrne and UBCSand	$(N_1)_{60}$	6.0	8.0	10.0	14.0	12.0
Byrne	C_1	0.93	0.65	0.49	0.32	0.39
Byrne	C_2	0.43	0.62	0.82	1.25	1.03
UBCSand	K^e_G	788.2	867.4	934.3	1045.1	992.8
UBCSand	K^e_B	1024.6	1127.6	1214.6	1358.6	1290.6
UBCSand	K^p_G	185.1	266.5	380.3	714.5	528.9
UBCSand	ne	0.5	0.5	0.5	0.5	0.5
UBCSand	me	0.5	0.5	0.5	0.5	0.5
UBCSand	np	0.4	0.4	0.4	0.4	0.4
UBCSand	$\phi_{cv}(^\circ)$	21.4	25.2	27.0	28.6	31.8
UBCSand	$\phi_p(^\circ)$	22.0	26.0	28.0	30.0	33.0
UBCSand	R_f	0.94	0.92	0.90	0.86	0.88

UBCSand models, but correlations with $(N_1)_{60}$ values (Byrne et al., 2004) was used to their estimates.

where υ is the Poisson ratio, E the Young's modulus, γ the unit weight, c' and ϕ′ the cohesion and the friction angle, respectively, n the porosity and k the coefficient of permeability.

where $(N_1)_{60}$ is the SPT value normalized to a overburden pressure of 100 kPa and corrected to 60% of the theoretical free fall hammer energy, C_1 (controls the amount of volume change) and C_2 (controls the shape of accumulated volume change with number of cycles) are constants of the Byrne model, K_G^e the elastic shear modulus factor in a reference level of 100 kPa, K_B^e the elastic bulk modulus factor in a reference level of 100 kPa, K_G^p the plastic shear modulus factor, ne the rate of stress-dependency of elastic shear modulus (default value 0.5), me the rate of stress-dependency of elastic bulk modulus (default value 0.5), np the rate of stress-dependency of plastic shear modulus, ϕ'_{cv} the constant volume friction angle, ϕ'_p the peak friction angle and R_f the failure ratio (default value 0.9).

3 SPT-BASED LIQUEFACTION TRIGGERING PROCEDURES

Simplified procedures for soil liquefaction triggering analysis were presented by Youd et al. (2001) and Boulanger & Idriss (2014). Estimation of two variables is required for evaluation of liquefaction resistance of soils: the cyclic resistance ratio (CRR), associated with the ability of soil to withstand liquefaction, and the cyclic stress ratio (CSR), associated with the seismic demand on the soil layer. Several field tests have gained common usage for evaluation of liquefaction resistance, including the standard penetration test (SPT). Criteria based on the SPT are largely embodied in the CSR versus $(N_1)_{60}$ plots where CRR curves are constructed to separate regions with data indicative of liquefaction and nonliquefaction regions. The cyclic resistance ratio (CRR) is affected by several corrections on $(N_1)_{60}$ values, including the effects of fines content, borehole diameter, rod length and correction for samplers with or without liners. Moreover, the base CRR curves apply only to earthquakes of magnitude 7.5 and, to adjust them to magnitudes smaller or larger than 7.5, a correction factor denoted as magnitude scaling factors (MSF) should be introduced, in order to scale the base curves upward or downward on CRR versus $(N_1)_{60}$ plots.

Seed and Idriss (1971) recommended the following equation for calculating the cyclic stress ratio (CSR) at depth z in the soil deposit, expressed in terms of an equivalent uniform value equal to 65% of the maximum cyclic shear stress ratio:

$$\mathrm{CSR} = 0.65 \times \left(\frac{\tau_{\max}}{\sigma'_{\mathrm{vo}}}\right) \tag{1}$$

where τ_{max} is the maximum earthquake induced shear stress and σ'_{v0} the in situ vertical effective stress.

The choice of the reference stress level (factor 0.65) was selected by Seed and Idriss (1967) and has been in use since, while the value of τ_{max} can be estimated from dynamic response analyses including a sufficient number of input acceleration time series and adequate site characterization of the geotechnical profile. In this research values of τ_{max} at several depths were calculated using the Shake2000 software (Ordoñez, 2011) considering the linear equivalent soil model for the response of the different soil layers along column 2 (Figure 1) in the tailings deposit.

The factor of safety (FS) against liquefaction is written in terms of CRR, CSR and MSF as follows:

$$\mathrm{FS} = \left(\frac{\mathrm{CRR}}{\mathrm{CSR}}\right) \times \mathrm{MSF} \tag{2}$$

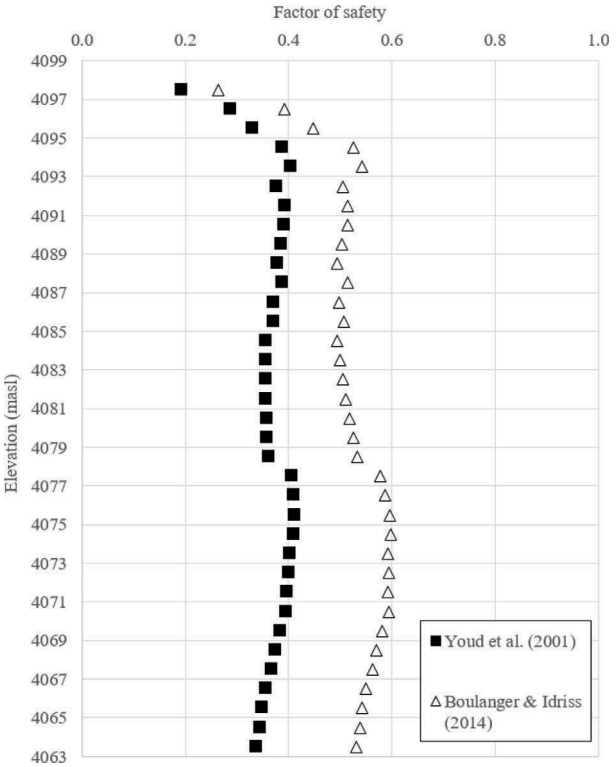

Figure 2. Distribution of the factors of safety along column 2 in the tailings deposit.

The distribution of the factors of safety along column 2 is shown in Figure 2. The results indicate liquefaction triggering in the tailings, thus requiring a numerical analysis to verify the global stability of the tailings dam.

4 NUMERICAL ANALYSIS

The numerical model was formed by 20,500 quadrilateral elements with maximum size of 5 m in order to ensure an adequate transmission of the SV waves through the finite difference mesh. Kuhlemeyer and Lysmer (1973) recommended a size less than 1/8 to 1/10 of the minimum wavelength within the geotechnical profile. The analysis was carried out in two stages: the first one for the incremental construction of the tailings dam and the determination of the steady state phreatic surface, while in the second stage the predominant frequencies of the different materials were determined and the dynamic behavior of the structure was investigated considering two different constitutive soil models for the liquefaction susceptible materials (Table 2). The Mohr-Coulomb model was adopted to represent the mechanical behavior of all the other materials (Table 1, except for rock considered linearly elastic) incorporating hysteretic damping through the linear equivalent model. The shear modulus reduction curves for gravels (Seed et al., 1986) and loose sands (Seed and Idriss, 1970) were used and the initial shear modulus (G_{max}) was considered varying as a function of the effective stress, following the suggestion given by Seed et al. (1986). A small percentage of Rayleigh damping (0.2% applied at the dominant frequency of the input record) was also introduced since it was observed (Han and Hart, 2006) that at very low cyclic strain levels the hysteretic damping provides no energy dissipation, so a small amount of stiffness-proportional Rayleigh damping was included to avoid low-level oscillations.

In this research, the definition of the pore pressure parameter r_u given by Beaty and Byrne (2011) has been used:

$$r_u = 1 - \left(\frac{\sigma'_v}{\sigma'_{vo}}\right) \tag{3}$$

where σ'_v is the current effective vertical stress and σ'_{v0} the initial effective vertical stress. When $r_u = 1$, $\sigma'_v = 0$ and the soil is in a liquefied state, but Beaty and Byrne (2011) suggested that values of r_u equal to or greater than 0.7 would already indicate the occurrence of dynamic liquefaction.

Figure 3 illustrates the regions where $r_u \geq 0.7$ at times t = 30 s and t = 198 s (total earthquake duration), from which it can be seen that at t = 30 s the liquefaction is restricted to the tailings located just below the surface, while at t = 198 s the liquefaction expanded significantly reaching the depth z = 30 m.

Figure 4 shows the position of several control points of r_u values, which were monitored along the time with the objective of verifying the evolution of the liquefaction potentials. As it can be observed in Figure 5 the UBCSand and Byrne constitutive models predicted the same results for ru-1 (no liquefaction for point situated within the dam body) and ru-16 (liquefaction for point situated next to the tailings deposit surface) but conflicting results appear for points ru-9 and ru-13 belonging to the new tailings layers.

Figure 6 shows the distribution of permanent displacements. In the tailings deposit the horizontal component reached 2.25 m and the vertical displacement component was 1.20 m (settlement), while in the dam the predicted horizontal displacement was 0.50 m, (downstream slope) and 0.50 m for settlement at the crest.

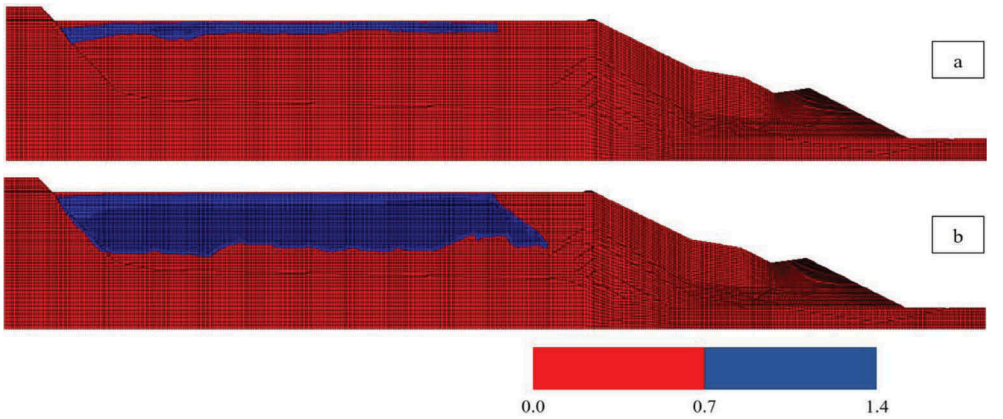

Figure 3. Distribution of parameter ru ≥ 0.7 at times (a) t = 30 s and (b) t = 198 s considering the UBC-Sand constitutive model.

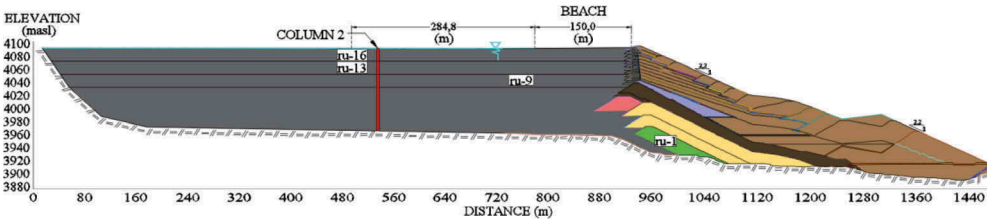

Figure 4. Position of the control points for ru values.

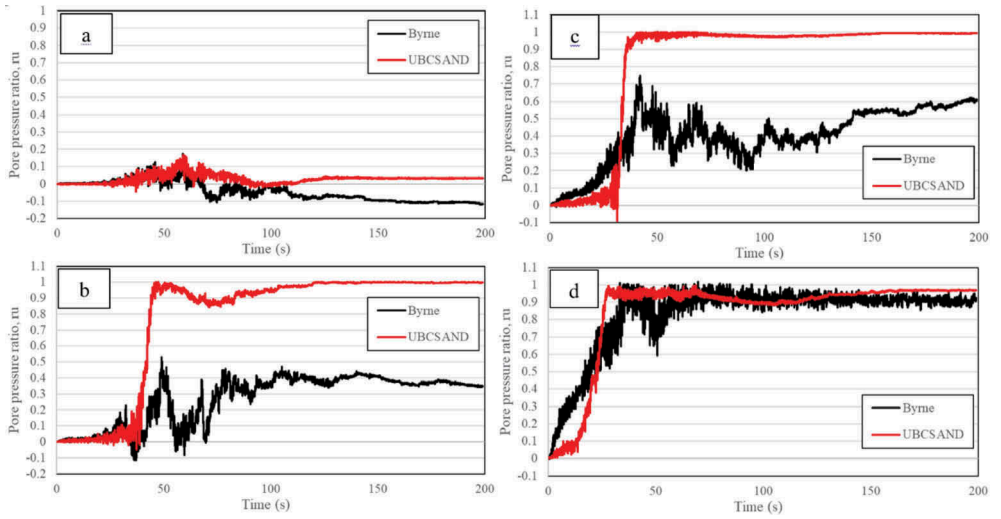

Figure 5. Evolution in time of the pore pressure parameter ru at points: (a) ru-1; (b) ru-9; (c) ru-13; (d) ru-16.

According to the recommendations of the California Geological Survey (2008) whenever the permanent displacement of a slope is between 10 and 100 cm, a careful analysis of stability, based on engineering judgment, should be carried out considering the risks associated with the possible collapse of the structure.

The response spectra were obtained from the previously calculated horizontal acceleration histories. Figure 7(a) shows the distribution of horizontal acceleration response spectra in some points of the dam body, which is mostly consisted of gravel. These spectra were determined including hysteretic damping and 0.2% Rayleigh damping. The response spectrum for the crest achieves the highest values of spectral acceleration, as can be observed.

For the tailings deposit, classified as silty sands, Figure 7(b) shows the horizontal acceleration response spectra, with the maximum values determined in the middle of the fine tailings layer.

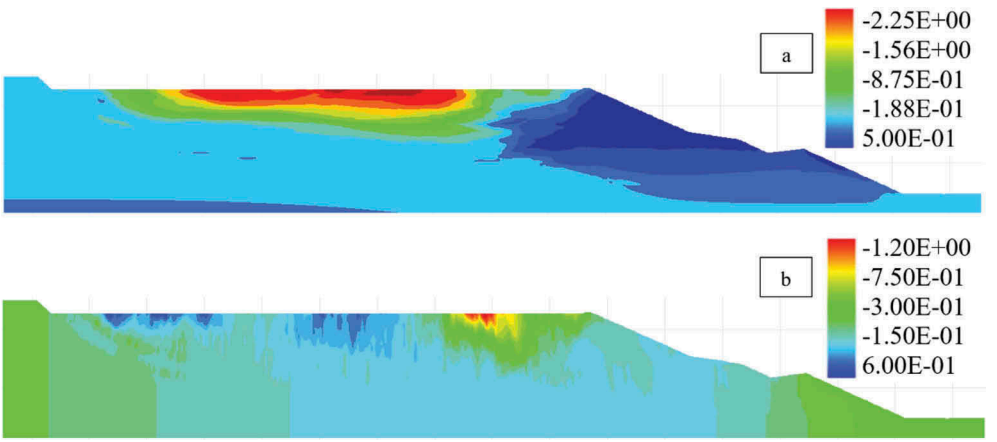

Figure 6. Permanent displacement distributions: (a) horizontal component; (b) vertical component.

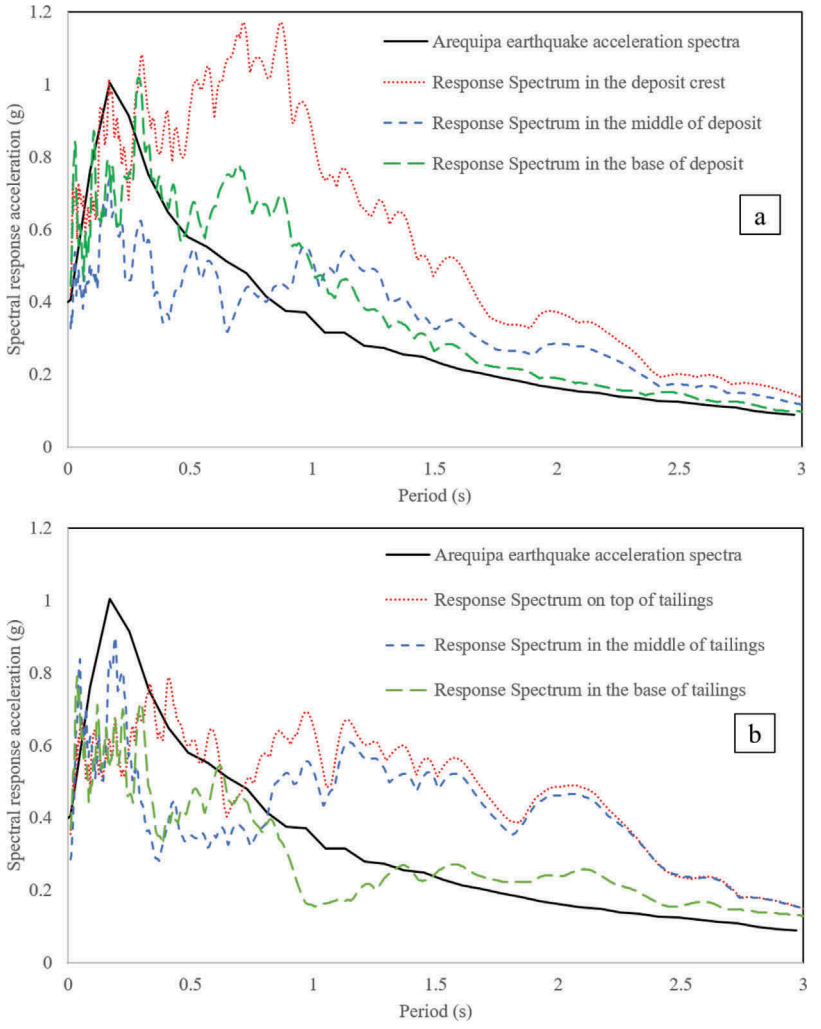

Figure 7. Horizontal acceleration response spectra: (a) dam; (b) tailings.

5 CONCLUSIONS

The main objective of this research was the evaluation of the dynamic liquefaction potential in a tailings dam located in Peru, in a region of high seismic activity. Two approaches were used: the first one based on the simplified methods of Youd et al. (2001) and Boulanger & Idriss (2014) for determining the factor of safety against dynamic liquefaction and, in the second approach, using a numerical model for a global analysis of the effects of the seismic loading in terms of permanent displacements, horizontal acceleration response spectra and pore pressure generation, considering the constitutive models of Byrne (1991) and UBCSand (2004). The safety evaluation earthquake (SEE) with a return period of 2475 years and peak horizontal acceleration PHA = 0.40 g was obtained from previous studies of seismic hazard by spectral adjustment of the Arequipa earthquake (M_w = 8.2).

The SPT-based simple procedures (Youd et al., 2001 and Boulanger & Idriss, 2014) are a practical and fast way for analysis of dynamic liquefaction triggering but the numerical model

permitted a global analysis of the seismic behavior of the dam and the tailings deposit in terms of dynamic liquefaction potential and of its consequences.

ACKNOWLEDGMENTS

This study was financed in part by the Coordenação de Aperfeiçoamento de Pessoal de Nível Superior - Brasil (CAPES) - Finance Code 001.

REFERENCES

Beaty, M.H. & Byrne, P.M. 2011. *UBCSand Constitutive Model Version 904aR*. Report UBCSand Constitutive Model on Itasca UDM Web Site. https://www.itascacg.com/udms/ubcsand/

Boulanger, R.W. & Idriss, I.M. 2014. *CPT and SPT based Liquefaction Triggering Procedures*. Report No. UCD/CGM-14/01, University of California, Davis.

Byrne, P.M. 1991. A Cyclic Shear-Volume Coupling and Pore Pressure Model for Sand, *Second International Conference on Recent Advances in Geotechnical Earthquake* Engineering *and Soil* Dynamics, *Proc., St. Louis*, *11-15 March*. Paper No. 1.24. Missouri.

Byrne, M.H. et al. 1995. Predicting Liquefaction Response of granular soils from self-boring pressumeter tests, *ASCE National Convention, San Diego*, *23-27 October*, 56: 122–135. California: ASCE.

Byrne, P.M. et al. 2004. Numerical modeling of liquefaction and comparison with centrifuge tests. *Canadian Geotechnical Journal* 41(2): 193–211.

California Geological Survey 2008. *Guidelines for evaluating and mitigating seismic hazards in California*: California Geological Survey Special Publication 117A: 98 p.

Canadian Dam Association 2013. *Dam Safety Guidelines 2007*. Edition 2013.

Han, Y. & Hart, R. 2006. Application of a simple hysteretic damping formulation in dynamic continuum simulations. In Hart & Varona (eds.), *4th International FLAC Symposium on Numerical Modeling in Geomechanics No. 04-02*, 29–31 *May*. Spain.

Harder, L.F. & Stewart, J.P. 1996. Failure of Tapo Canyon Tailings Dam. *Journal of Performance of Constructed Facilities, ASCE*, 10(3): 109–114.

Itasca 2016. *FLAC, Fast Lagrangian Analysis of Continua, Version 8.0*. Itasca Consulting Group, Minneapolis, MN. https://www.itascacg.com/

Kuhlemeyer, R.L. & Lysmer, J. 1973. Finite element accuracy for wave propagation problems. *Journal of the Soil Mechanics and Foundations Division*, 99(5): 421–427.

Mantegh, A. 2006. *Evaluation of liquefaction potential of mine tailings using elastic wave velocity*. PhD Thesis, Department of Mining, Metals and Materials Engineering, McGill University, Montreal, Canada.

Ordoñez, G. 2011. *Shake2000: a computer program for the 1D analysis of geotechnical earthquake problems*.

Seed, H.B. & Idriss, I.M. 1967. *Analysis of liquefaction: Niigata earthquake*. Proceedings, ASCE, 93 (SM3), 83–108.

Seed, H.B. & Idriss, I.M. 1970. *Soil Moduli and damping factors for dynamic response analysis*. Report No. EERC 70-10, University of California, Berkeley.

Seed, H.B. & Idriss, I.M. 1971. Simplified procedure for evaluating soil liquefaction potential. *Journal of the Soil Mechanics and Foundations Divisions*, 97(SM9): 1249–1273.

Seed, H.B. et al. 1986. Moduli and damping factors for dynamic analyses of cohesionless soils. *Journal of Geotechnical Engineering, ASCE*, 112(11): 1016–1032.

Tavera, H. 2002. *Proceso de ruptura del terremoto de Arequipa del 23 de junio 2001 y de tres de sus réplicas de magnitud mayor (resultados preliminares)*. Reporte: El terremoto de región sur de Perú del 23 de junio de 2001, Centro Nacional de Datos Geofísicos, Lima.

Venegas, F.J. 2011. *Análisis de respuesta sísmica reciente en balsas de relaves chilenas y presas de material suelto*. Trabajo de Fin de Máster, Máster en Ingeniería de las Estructuras, Cimentaciones y Materiales, Escuela de Caminos, Canales y Puertos, Universidad Politécnica de Madrid, España.

Verdugo, R. & González, J. 2015. Liquefaction-induced ground damages during the 2010 Chile earthquake. *Soil Dynamics and Earthquake Engineering, Elsevier*, 79: 280–295.

Youd, T.L. et al. 2001. Liquefaction Resistance of soils: Summary Report from the 1996 NCEER and 1998 NCEER/NSF Workshops on Evaluation of Liquefaction Resistance of Soils. *Journal of Geotechnical and Geoenvironmental Engineering, ASCE*, 127(10): 817–833.